Arch Toxicol (2015) 89:979–990
DOI 10.1007/s00204-014-1283-x

PROTOCOLS

Sandwich-cultured rat hepatocytes as an in vitro model to study canalicular transport alterations in cholestasis

Gisel S. Miszczuk · Ismael R. Barosso · Andrés E. Zucchetti · Andrea C. Boaglio · José M. Pellegrino · Enrique J. Sánchez Pozzi · Marcelo G. Roma · Fernando A. Crocenzi

Received: 24 January 2014 / Accepted: 20 May 2014 / Published online: 10 June 2014

Abstract At present, it has not been systematically evaluated whether the functional alterations induced by cholestatic compounds in canalicular transporters involved in bile formation can be reproduced in sandwich-cultured rat hepatocytes (SCRHs). Here, we focused on two clinically relevant cholestatic agents, such as estradiol 17β-D-glucuronide (E17G) and taurolithocholate (TLC), also testing the ability of dibutyryl cyclic AMP (DBcAMP) to prevent their effects. SCRHs were incubated with E17G (200 μM) or TLC (2.5 μM) for 30 min, with or without pre-incubation with DBcAMP (10 μM) for 15 min. Then, the increase in glutathione methyl fluorescein (GS-MF)-associated fluorescence inside the canaliculi was monitored by quantitative time-lapse imaging, and Mrp2 transport activity was calculated by measuring the slope of the time-course fluorescence curves during the initial linear phase, which was considered to be the Mrp2-mediated initial transport rate (ITR). E17G and TLC impaired canalicular bile formation, as evidenced by a decrease in both the bile canaliculus volume and the bile canaliculus width, estimated from 3D and 2D confocal images, respectively. These compounds decreased ITR and induced retrieval of Mrp2, a main pathomechanism involved in their cholestatic effects. Finally, DBcAMP prevented these effects, and its well-known choleretic effect was evident from the increase in the canalicular volume/width values; this choleretic effect is associated in part with its capability to increase Mrp2 activity, evidenced here by the increase in ITR of GS-MF. Our study supports the use of SCRHs as an in vitro model useful to quantify canalicular transport function under conditions of cholestasis and choleresis.

Keywords Sandwich-cultured rat hepatocytes · Mrp2 · Initial transport rate · Transporter retrieval · Dibutyryl cAMP · Canalicular volume

G. S. Miszczuk · I. R. Barosso · A. E. Zucchetti · A. C. Boaglio · J. M. Pellegrino · E. J. Sánchez Pozzi · M. G. Roma · F. A. Crocenzi (✉)
Instituto de Fisiología Experimental (IFISE) - Consejo Nacional de Investigaciones Científicas y Técnicas (CONICET), Facultad de Ciencias Bioquímicas y Farmacéuticas – Universidad Nacional de Rosario (UNR), Suipacha 570, S2002LRL Rosario, Argentina
e-mail: crocenzi@ifise-conicet.gov.ar

Introduction

Hepatocellular cholestasis results from any condition primarily affecting the ability of hepatocytes to produce bile. Agents able to induce hepatocellular cholestasis include drugs, hormones and cytokines (Roma et al. 2008). Changes in transporter expression, activity or localization may represent the primary causal factor of the cholestatic dysfunction. Bile flow can be impaired within minutes by endocytosis of canalicular transporters from their membrane domain to an endosomal compartment (Crocenzi et al. 2012).

The need to study these rapid changes in hepatocyte transport function in a rapid and reproducible manner, avoiding the use of experimental animals, has encouraged the development of in vitro, polarized models of hepatocellular transport. For example, isolated rat hepatocyte couplets (IRHCs) have been successfully used since the early 1980s to study structural alterations (cytoskeleton, tight junctions), impairment in function and localization of transporters induced by toxic and/or cholestatic compounds, and their prevention by hepatoprotective compounds (Coleman and Roma 2000; Milkiewicz et al. 2002b; Roma et al. 2008). Administration of either the endogenous estradiol

metabolite estradiol-17ß-D-glucuronide (E17G) (Crocenzi et al. 2003a, 2008) or the monohydroxylated bile salt taurolithocholate (TLC) (Crocenzi et al. 2003b; Milkiewicz et al. 1999) to IRHCs induces acute cholestasis, accompanied with endocytic internalization of the canalicular transporters Mrp2 and Bsep and the associated impairment in transport function, in line with the acute cholestatic effects of these cholestatic agents in vivo (Crocenzi et al. 2003a, b; Mottino et al. 2002). These findings have potential clinical relevance, since E17G has been implied as a key metabolite involved in pregnancy-induced cholestasis (Vore et al. 1997), whereas TLC was proposed to play a role in the liver dysfunction occurring in primary biliary cirrhosis (Murphy et al. 1972), progressive familial intrahepatic cholestasis (Linarelli et al. 1972), total parenteral nutrition-induced cholestasis (Fouin-Fortunet et al. 1982), and neonatal cholestasis (Setchell et al. 1998).

Dibutyryl cyclic AMP (DBcAMP) was shown to stimulate the targeting of transporters to the canalicular membrane (Kipp et al. 2001; Roelofsen et al. 1998; Roma et al. 2000), and to counteract the impairment in apical secretory function and retrieval of canalicular transporters induced by both TLC (Crocenzi et al. 2003b; Milkiewicz et al. 2002a) and E17G (Crocenzi et al. 2003a, 2005; Mottino et al. 2002), both in vivo and in IRHCs. As a consequence of its ability to stimulate insertion of canalicular transporter-containing vesicles into the apical domain, DBcAMP can also increase the circumference, and therefore the volume, of canalicular vacuoles in IRHCs (Boyer and Soroka 1995).

It has become progressively apparent that both E17G and TLC induce cholestatic alterations by activation of several intracellular signaling pathways (Barosso et al. 2012; Beuers et al. 1999, 2003; Boaglio et al. 2010, 2012; Crocenzi et al. 2008; Schonhoff et al. 2013; Zucchetti et al. 2013). Evaluation of the nature of these signaling pathways requires time-lapse activation studies (by enzyme activity tests or Western blot). However, this requires amounts of protein hard to obtain from IRHCs, due to the relatively low yield per preparation. In addition to evaluate the role of a signaling pathway by measuring its activation, or the effect of its inhibition using specific chemicals inhibitors, more direct evidences are required nowadays, for example knockdown of the gene encoding the candidate signaling molecule using *state-of-the-art* interference RNA technology. However, gene knockdown studies are usually carried out between 48 and 72 h after cell transfection with the respective interference RNA. This makes IRHCs useless, since they preserve functionality for approximately 10 h (Wilton et al. 1993). Thus, an alternative polarized hepatocellular model, based upon primary cultured hepatocytes to better reproduce physiological conditions, which bears longer stability and higher protein yield than IRHCs, needs to be established and validated for functional studies of cholestasis in vitro.

Isolated hepatocytes, when cultured in between two layers of gelled collagen, i.e., in sandwich configuration, acquire a morphology that resembles that present in vivo, including the formation of intact canalicular networks, with physiological secretion levels of many liver-specific proteins and organic compounds, like urea, albumin and bile acids, as first demonstrated by Dunn et al. (1989, 1991, 1992). In addition, a conserved expression of membrane transporters crucial for uptake and canalicular excretion of bile salts (Ntcp and Bsep, respectively) and non-bile salt organic anions (Oatps and Mrp2, respectively) was described up to 4 days of culture in sandwich-cultured rat hepatocytes (SCRHs) (Swift et al. 2010). Due to the conserved transport and metabolism of endogenous and exogenous compounds, this model was further employed for the study of hepatic clearance of xenobiotics, drug–drug interactions and drug-induced hepatotoxicity (De Bruyn et al. 2013).

Two different methodologies have been described and applied for the study of canalicular transport in SCRHs. One is based on the calculation of the biliary excretion index (BEI) of radioactive or fluorescent canalicular transporter substrates, by measuring the difference between the amount of fluorescent/radioactive compound accumulated in the whole culture (cells plus bile canaliculi) and the amount of compound retained after exposure to a Ca^{2+}-free medium to impair tight junctions and to allow for the release of the canalicular content. This requires two identically treated culture wells per single preparation to be differentially exposed to a Ca^{2+}-containing or a Ca^{2+}-free buffer medium, followed by homogenization of the cells, measurement of the fluorescence or radioactivity present in the supernatant and finally, calculation of BEI (Liu et al. 1999). By using this approach, the well-known capability of certain drugs to impair bile acid transport, such as cyclosporine A and glyburide, could be confirmed in the SCRH model (Ansede et al. 2010).

However, this method has important drawbacks that complicate and even preclude its use for bile formation studies, namely:

1. The method is cumbersome, since it has a number of steps including extraction from the culture homogenate and the further spectrofluorescence or radioactivity quantification of the tested substrate.
2. Reproduction of the results is difficult, because of potential sources of heterogeneity of the culture features in both wells (e.g., differential growth pattern, attachment, etc.) and chiefly, methodological errors associated with the multiple steps required.

3. The potential perturbation produced by the changes in extracellular Ca^{2+} levels when signaling-dependent events are evaluated, due to the well-recognized properties of Ca^{2+} as a signaling molecule itself.

An alternative, more direct and less time-consuming method has been proposed recently and proved successful to measure Bsep- (Kruglov et al. 2011) and Mrp2-mediated (Cruz et al. 2010) transport processes. It requires monitoring the increase with time of the fluorescence associated with a specific fluorescent substrate into the canaliculi by quantitative time-lapse imaging (QTLI), with the aid of an inverted fluorescence microscope (Nakanishi et al. 2011). Nakanishi et al. (2011) have pointed two main reasons to consider this method superior to BEI measurement, namely (1) extraction of the substrate tested from cell homogenate and quantification of their concentration is unnecessary and (2) apical fluorescence accumulation can be monitored over time in all the bile canaliculi present on a microscopy field in a single well.

At present, it has not been systematically evaluated whether the functional alterations induced by cholestatic compounds in canalicular transporters involved in bile formation, and its reversion by anticholestatic agents, can be reproduced in SCRHs. Therefore, the aim of this work was to validate the use of SCRHs as a model for cholestasis studies, focusing on two clinically relevant cholestatic agents, such as TLC and E17G, and their effect on Mrp2 localization and transport function. Additionally, the ability of DBcAMP to prevent these cholestatic effects in SCRHs was tested. Finally, we have focused on the effect of the cholestatic compounds and the DBcAMP treatment on canalicular volume, and the possible influence of changes in this parameter on the quantification of the Mrp2-dependent transport process.

Materials and methods

Chemicals

Estradiol 17β-D-glucuronide (E17G), taurolithocholic acid (TLC), collagenase type A (from *Clostridium histolyticum*), bovine serum albumin, L-15 culture medium, dimethyl sulfoxide (DMSO), Triton X-100, paraformaldehyde, N6,2′-*O*-dibutyryladenosine 3′:5′-cyclic monophosphate (DBcAMP) and urethane were acquired from Sigma Chemical Co. (St. Louis, MO). 5-Chloromethylfluorescein diacetate (CMFDA) was obtained from Molecular Probes (Eugene, OR). Mouse antihuman MRP2 (M2III-6) was obtained from Alexis Biochemicals (San Diego, CA). Anti-mouse IgG (31430) was obtained from Thermo Fisher Scientific, Inc. (Waltham, MA). Dulbecco's modified Eagle's medium (DMEM), Alexa Fluor 568 phalloidin and 4,6-diamidino-2-phenylindole were acquired from Invitrogen (Carlsbad CA). Cy2-labeled goat anti-mouse IgG was from Zymed (San Francisco, USA). All other chemicals were of the highest grade available.

Animals

Adult female Wistar rats weighing 250–300 g under urethane anesthesia (1 g/kg, intraperitoneally) were used in all studies. All animals received humane care according to the criteria outlined in the "Guide for the Care and Use of Laboratory Animals" Eighth Edition, National Academy of Sciences. Experimental procedures were carried out according to the local Guideline for the Use of Laboratory Animals (Resolution No. 6109/012, Faculty of Biochemical and Pharmaceutical Sciences, National University of Rosario, Argentina).

Isolation and culture of SCRHs

Hepatocytes were isolated as described previously (Garcia et al. 2001). Every well of six-well plastic culture plates was covered with 800 µL of rat tail collagen type I (5 mg/mL), dissolved in 0,02 N acetic acid, mixed with 100 µL of DMEM 10X, and adjusted to pH 7,4 with 0.2 N NaOH (approx. 100 µL). Isolated hepatocytes were plated at a density of 1.3 to 1.5 × 10^5 cells/cm^2 and incubated for 2 h, to allow the cells to attach, at 37 °C, 95 % O_2/5 % CO_2 in DMEM medium with FBS 5 %, containing antibiotics (gentamicin, streptomycin, penicillin and amphotericin D), dexamethasone (0.8 mg/L) and insulin (100 U/L). Thereafter, the medium was replaced by fresh one to remove cellular detritus and death cells. Then, the medium was replaced every 24 h.

Twenty-four hours later, the medium was removed and collagen was overlaid on the cells (120 µL of the preparation described above, gently added drop by drop). The SCRHs were incubated for 1 h under a 5 % CO_2/95 % air mixture, at 37 °C, and then DMEM with the supplements indicated above was added. The culture was continued for 48 h under 5 % CO_2/95 % air mixture at 37 °C, to obtain a collagen-sandwich configuration, as previously described (Barosso et al. 2012).

SCRHs treatments

Sandwich-cultured rat hepatocytes were incubated in L-15 with E17G (25–200 µM), TLC (1–2.5 µM), or vehicle (DMSO) in controls, at 37 °C for 30 min. To assess the ability of DBcAMP to prevent the effects of E17G and TLC, SCRHs were pre-incubated with DBcAMP (10 µM) for 15 min. Then, TLC (2.5 µM) or E17G (200 µM) were added, and cells were incubated for another 30-min period.

Assessment of Mrp2 secretory function in SCRHs

After treatments, plates containing the SCRHs were placed on an inverted fluorescence microscope (Zeiss Axiovert 25), over a plate thermostated at 37 °C. Then, the SCRHs were washed, and CMFDA, a metabolic precursor of the fluorescent substrate of Mrp2 glutathione methyl fluorescein (GS-MF), was added to L-15, so as to reach a final concentration of 2.5 μM. QTLI was performed to observe the fluorescence of GS-MF accumulated in the bile canaliculi for up to 8 min after CMFDA addition. 12-bit images were taken every 1 min with an exposure time of 200 ms and a lens of 10×, using an attached digital camera (Olympus QColor5).

Image analysis was carried out using ImageJ software. In order to correct subtle displacement between images, each series of images were aligned with the StackReg (Rigid Body) plugin. Regions of interest (ROIs) of 2 × 2 pixels were selected inside every canaliculus present in the visual field, and the fluorescence intensities obtained from 80 to 120 ROIs in each image were averaged per pixel, using the Stacks-T-Function (Time Series Analyzer) plugin. The mean fluorescence value from all the ROIs was used to quantify canalicular accumulation of GS-MF in each image. The fluorescence values were plotted against time, and a linear regression analysis was carried out using values obtained from time 0 to 4 min, i.e., the time window where canalicular fluorescence showed a linear increment. Slope of the linear regression curves was considered to be the Mrp2-mediated initial transport rate (ITR).

Assessment of Mrp2 localization in SCRHs by confocal microscopy

To evaluate the intracellular distribution of Mrp2, a different set of SCRHs belonging to the same SCRH preparations used for Mrp2 transport function was incubated with E17G (200 μM), TLC (2.5 μM), or vehicle in controls (DMSO), with or without pre-treatment with DBcAMP (10 μM). After this, SCRHs were fixed with 4 % paraformaldehyde in PBS for a 30-min period, blocked and permeabilized with 3 % bovine serum albumin and 0.5 % Triton X-100 for another 30-min period. Then, cells were incubated with a mouse monoclonal antibody against human MRP2 (1:200) overnight at 4 °C, followed by incubation with a Cy2-labeled goat anti-mouse IgG (1:100, 2 h). To delimit the canaliculi, F-actin was stained by coincubating cells with Alexa Fluor 568 phalloidin (1:100, 2 h). Cellular nuclei were stained by incubating during 10 min with 1.5 mM 4,6-diamidino-2-phenylindole. Finally, cells were mounted and examined with a Nikon C1 Plus confocal laser scanning system attached to a Nikon TE-2000 inverted microscope. All samples were coded and scored according to morphological criteria (canalicular presence, canalicular length per cell). At least five imaged areas of confluent cells were randomly selected from each culture dish.

Estimation of canalicular volume in SCRHs

Measurement of the average canalicular volume and its putative surrogate parameter, canalicular width, were performed in each SCRH preparation, to account for morphological heterogeneity among different preparations.

The average canalicular width of each SCRH preparation was carried out as a first approach to correct for distortions in fluorescence intensity induced by changes in canalicular volume induced by the treatments. For this purpose, the average width of 40 canaliculi assessed in 2D confocal images of F-actin staining, where canalicular limits can be visualized, was measured using the imaging software NIS-Elements Ar 4.0 (Nikon Instruments Inc.).

In addition, to estimate the actual canalicular volume, 3D stacks of F-actin-stained confocal images were builded with the Stack Building plugin of the ImageJ software. Threshold was adjusted to clearly detect Alexa Fluor 568 phalloidin-dependent fluorescence, and Particle Analysis (Object Counter3D) plugin was applied to estimate the canalicular volume.

Statistical analysis

Results are expressed as mean ± standard error of the mean (SEM). One-way ANOVA, followed by Newman–Keuls' test, was used for multiple comparisons. Values of $p < 0.05$ were considered to be statistically significant.

Results

Initial transport rate (ITR) is a sensitive parameter to detect changes in Mrp2-mediated transport induced by E17G, TLC and DBcAMP

Figure 1a shows representative images of the time-dependent increase in GS-MF-associated fluorescence inside the canaliculi of SCRHs under control conditions, or after incubation with the cholestatic compound E17G. Alterations in the canalicular transport mediated by Mrp2 can be visualized as a delay in the appearance of intracanalicular GS-MF-associated fluorescence; whereas fluorescence signal was already visible by 2 min after addition of CMFDA in controls, it took an additional minute to become detectable after treatment with the cholestatic compound.

Temporal changes in the average fluorescence accumulated in the canaliculi are shown in Fig. 1b. ITR was

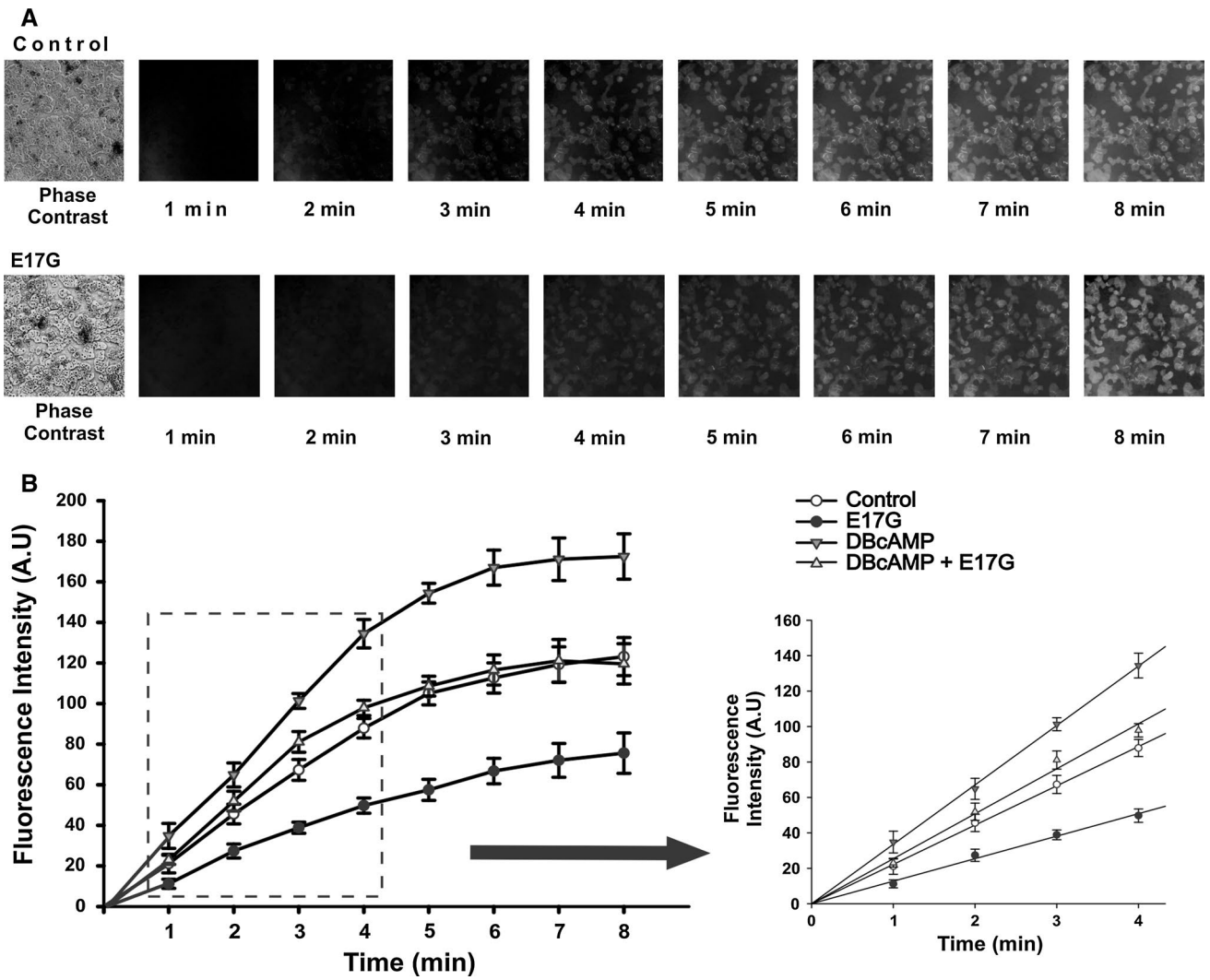

Fig. 1 **a** Representative time-lapse images of GS-MF transport, taken every minute, in control SCRHs and in SCRHs exposed to E17G (200 μM, 30 min) after the addition of CMFDA (2.5 μM). Note the delay in the appearance of GS-MF-associated fluorescence inside the canaliculi of SCRHs exposed to the cholestatic compound. **b** Representative curves of canalicular fluorescence intensity associated with GS-MF versus time after CMFDA addition. The curve was obtained by plotting the average of GS-MF-associated canalicular fluorescence versus time. The average of fluorescent intensity at each time was estimated by using the ImageJ software. SCRHs were exposed to either vehicle (DMSO, control), DBcAMP (10 μM, 15 min), or E17G (200 μM, 30 min), in the presence or absence of a pre-treatment with DBcAMP (10 μM, 15 min). About 70–100 canaliculi were selected per image ($n = 6$, from three independent SCRH preparations) to calculate the average fluorescence intensity. In order to calculate the transport activity of Mrp2, the points of the curves where GS-MF-associated fluorescence increased linearly (1–4 min) were selected (demarcated zone), and the curves adjusted by linear regression ($r^2 > 0.98$, $p < 0.001$, right graph). The slope of the regression curves was referred to as *initial transport rate* (ITR) of GS-MF

calculated as the slope of the regression curves, taking into account the points of the curve where the fluorescence increments show a linear pattern (from 1 to 4 min, demarcated zone in the left panel). The graph on the right panel shows the regression curves calculated with points within this time window; E17G induced a clear decrease in the slope of the regression curve, which was normalized by pre-incubation with DBcAMP, compound that increased per se this parameter.

Concentration–response studies were carried out by varying the concentration of the cholestatic compound in the incubation medium (25–200 μM for E17G, and 1–2.5 μM for TLC). Both E17G (Fig. 2a) and TLC (Fig. 2b) significantly decreased ITR of GS-MF from a concentration of 50 and 1.5 μM onwards, respectively. Further increments in the concentration of both E17G and TLC resulted in a trend toward a higher decrease in ITR, although it did not reach statistical significance.

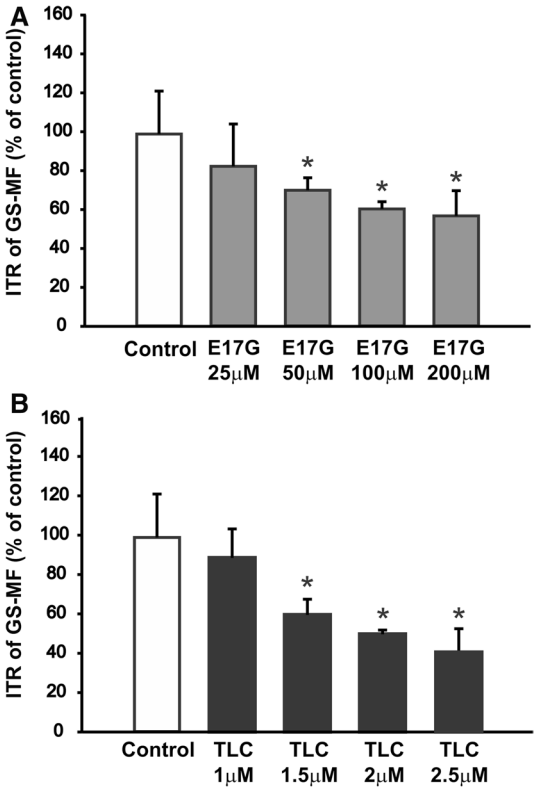

Fig. 2 Concentration–response effect of E17G and TLC on GS-MF canalicular transport. SCRHs were exposed to different concentrations of E17G (25–200 μM, **a**) or TLC (1–2.5 μM, **b**) for 30 min. The slope of the curve obtained by plotting the average GS-MF-associated fluorescence of 70–100 canaliculi versus time was used to estimate the ITR of GS-MF, a measure of Mrp2 transport activity. ITR values were expressed as percentage of control values ($n = 6$, from three independent SCRH preparations). $^*p < 0.05$ versus control

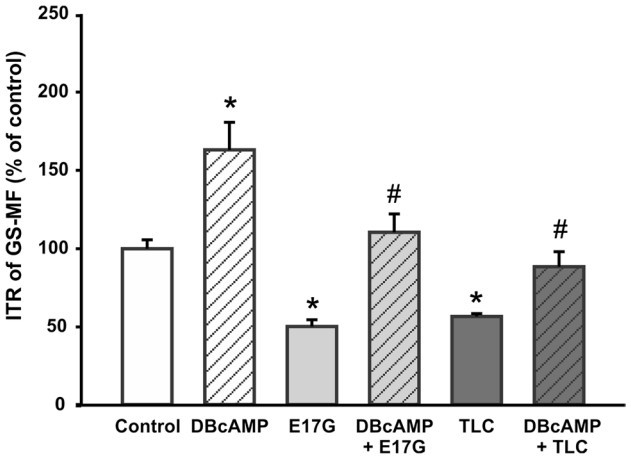

Fig. 3 DBcAMP increases ITR of GS-MF and prevents E17G- and TLC-induced decrease of this parameter. SCRHs were pre-incubated with 10 μM DBcAMP for 15 min and then exposed to 200 μM E17G or 2.5 μM TLC for another 30 min. The slope of the curve obtained by plotting the average GS-MF-associated fluorescence of 70–100 canaliculi versus time was used to estimate ITR of GS-MF, a measure of Mrp2 transport activity. ITR values were expressed as percentage of control values ($n = 6$, from three independent SCRH preparations). $^*p < 0.05$ versus control; $\#p < 0.05$ versus the respective cholestatic group

From the statistical analysis of the slopes of the regression curves for each experimental group (ITR values) shown in Fig. 3, it becomes apparent that ITR properly reflects the expected changes in Mrp2 transport function in response to the different treatments. Indeed, this parameter is decreased by E17G, a cholestatic compound that induces rapid endocytic internalization of Mrp2 both in vivo (Mottino et al. 2002) and in IRHCs (Crocenzi et al. 2005). On the other hand, ITR increased in response to treatment with DBcAMP, a finding in line with the well-established property of cAMP to stimulate the quick sorting of Mrp2 to the apical domain (Kipp et al. 2001; Roelofsen et al. 1998; Roma et al. 2000). Finally, pre-treatment with DBcAMP fully prevented the decrease in ITR induced by E17G, a finding in line with the capability of DBcAMP to counteract E17G-induced Mrp2-dependent transport function both in vivo (Mottino et al. 2002) and in IRHCs (Crocenzi et al. 2005). A similar decrease in ITR to that induced by E17G was recorded after incubation of SCRHs with the cholestatic agent TLC, which was also prevented by pre-treatment with DBcAMP. Again, these changes correlate well with previous reports showing that TLC acutely impairs Mrp2 transport function both in vivo (Roma et al. 1994) and in IRHCs (Crocenzi et al. 2005; Milkiewicz et al. 1999, 2002a).

The DBcAMP-dependent increment in ITR of GS-MF and the DBcAMP-mediated prevention of E17G- and TLC-induced deleterious effects on this parameter are associated with changes in Mrp2 localization

Previous studies by our group and others on the cholestatic effects of E17G and TLC both in vivo (Mottino et al. 2002), in IPRL (Beuers et al. 2001) and in IRHCs (Crocenzi et al. 2005), as well as its prevention by DBcAMP, showed that the degree of Mrp2 endocytic internalization consistently reflected Mrp2 transport activity. To ascertain whether the changes in Mrp2 transport function, as evaluated by ITR of GS-MF, also reflect changes in Mrp2 localization in the SCRH model, the effect of E17G and TLC, in the presence or absence of DBcAMP, on Mrp2 localization, was evaluated by immunostaining followed by confocal microscopy. Figure 4 shows confocal images of SCRHs stained for Mrp2 under the different treatments. F-actin was also stained to demarcate the limits of the canalicular membrane, since actin network exhibits a predominant pericanalicular distribution in polarized hepatocytes (Tsukada et al. 1995). The image in the control group confirmed that

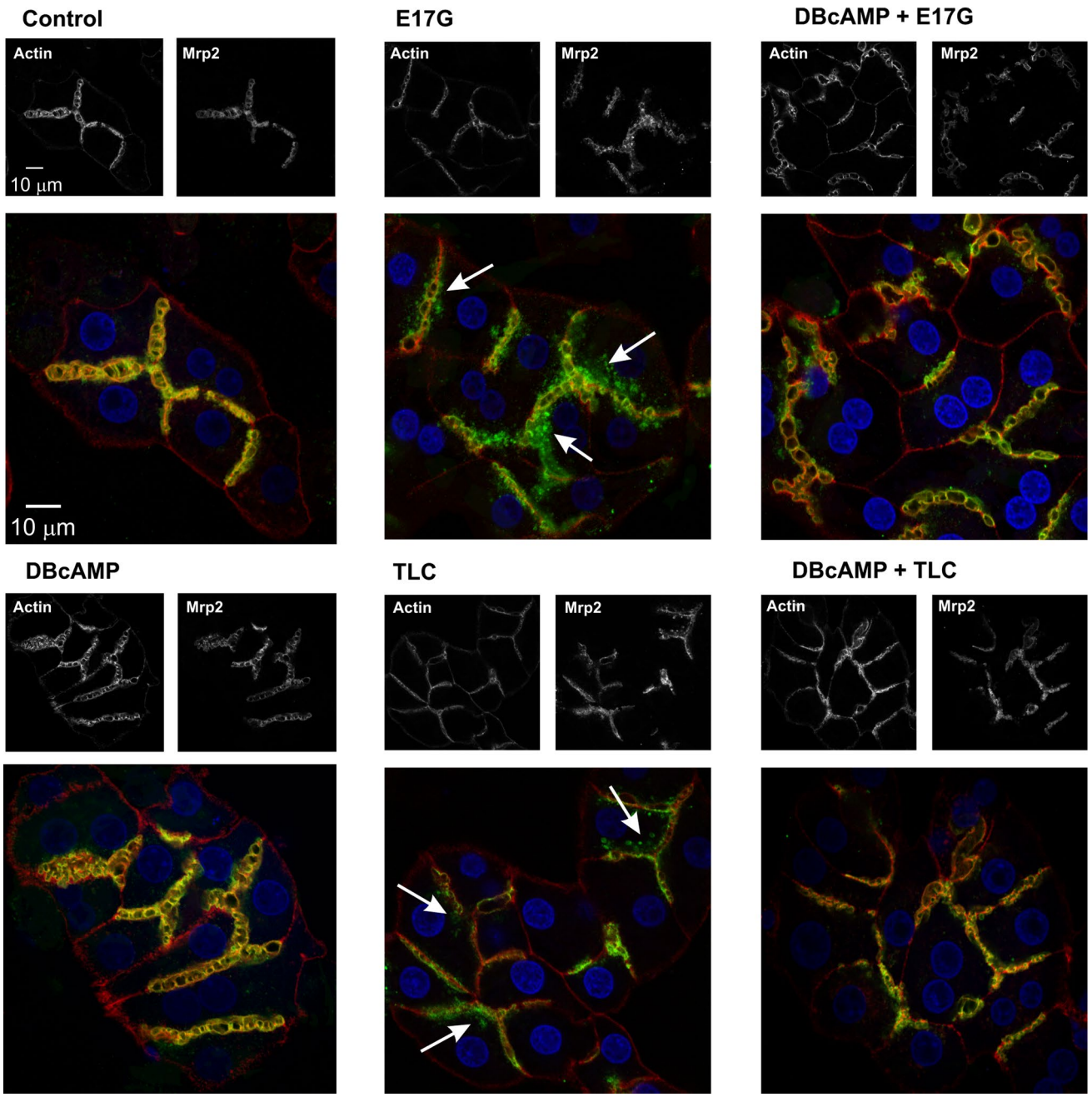

Fig. 4 DBcAMP prevents E17G- and TLC-induced endocytic internalization of Mrp2 in SCRHs. Representative confocal images showing cellular distribution of Mrp2, F-actin, and merged images (with F-actin in *red* and Mrp2 in *green*) in SCRHs under the different treatments. Nuclei (*blue*) are also shown in merged images. Note that under control conditions, Mrp2-associated fluorescence is mainly localized at the canalicular membrane in the area delimited by the pericanalicular actin network. The cholestatic compounds, E17G (200 μM) and TLC (2.5 μM), induced a clear internalization of Mrp2-containing vesicles beyond the limits of the pericanalicular actin (*white arrows*); this phenomenon was significantly prevented by pre-incubation with 10 μM DBcAMP. None of the treatments affected the normal distribution of F-actin, which showed a predominant pericanalicular distribution (color figure online)

Mrp2 was mainly confined within the canalicular space. SCRHs treated with DBcAMP exhibited the same distribution pattern. On the other hand, treatments with E17G and TLC-induced retrieval of Mrp2 from the canalicular membrane into the endosomal compartment, as indicated by the presence of Mrp2-containing intracellular vesicles. Pre-treatment of SCRHs with DBcAMP prevented this relocalization.

Table 1 Changes in canalicular width and volume of SCRHs induced by the different treatments

	Canalicular width (μm)	Canalicular volume (μm^3)
Control	2.9 ± 0.2	4,587 ± 493
DBcAMP	4.0 ± 0.2*	7,113 ± 562*
E17G	2.4 ± 0.1*	2,743 ± 247*
E17G+DBcAMP	3.2 ± 0.1#	4,295 ± 345#
TLC	2.5 ± 0.1*	3,250 ± 281*
TLC+DBcAMP	3.3 ± 0.2#	4,579 ± 181#

The canalicular width was estimated by NIS-Elements Ar 4.0 software on 2D confocal images, and the estimation of the canalicular volume was carried out by ImageJ software on 3D stacks. Between 20 and 30 canaliculi per experimental group were measured, from three independent preparations

* $p < 0.05$ versus control

# $p < 0.05$ versus E17G or TLC

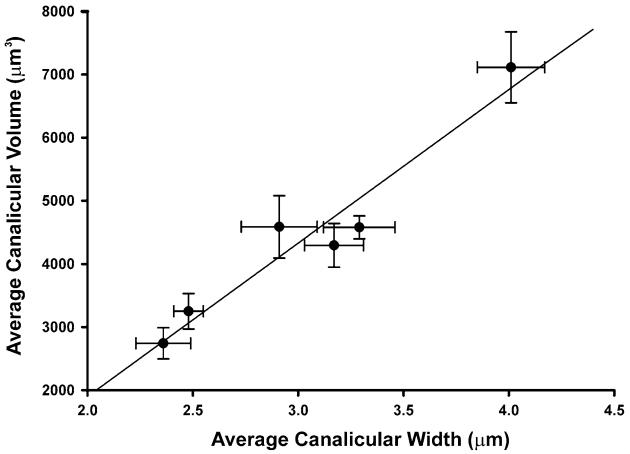

Fig. 5 Correlation between canalicular volume and canalicular width. The data shown in Table 1 of canalicular width and canalicular volume estimation in the different experimental groups were plotted, and a regression analysis was performed. Between 20 and 30 canaliculi per experimental group were measured, from three independent preparations. Data are expressed as mean ± SEM. A tight correlation was recorded ($r^2 = 0.92$, $p < 0.002$)

The different treatments modify the bile canaliculus width and volume on SCRHs

Since canaliculi in SCRHs are sealed spaces with no drainage way, changes in bile formation should be reflected in changes in their average volume; this relationship was confirmed in other hepatocellular polarized models such as IRHCs (Gautam et al. 1989) and HepG2 cultured cells (Larocca et al. 2009) which, like SCRHs, exhibit a sealed luminal space. Furthermore, such a phenomenon was successfully employed to quantify canalicular bile formation in vitro. This prompts us to ascertain whether this holds true for the SCRH model as well.

Estimation of actual canalicular volume in SCRHs is somewhat laborious, since it requires acquisition of 3D confocal images and a computer-assisted 3D reconstruction of the canaliculi. On the contrary, assessment of the average canalicular width is more approachable, since it can be easily calculated from conventional 2D confocal images. Therefore, we evaluated the feasibility of using average canalicular width as a surrogate parameter of the canalicular volume for rapidly quantifying changes in canalicular bile formation in the SCRH model.

As shown in Table 1, exposure to DBcAMP resulted in a significant increase in both parameters, while both E17G and TLC induced a significant drop of them. Finally, pretreatment with DBcAMP completely prevented E17G- and TLC-induced impairment of both parameters.

A highly significant correlation was obtained when average canalicular volume and average canalicular width were correlated ($r^2 = 0.92$; $p < 0.002$) (Fig. 5). From these results, it is apparent that either of both parameters can be used to estimate canalicular bile formation in the SCRH model and support the use of the average canalicular width as an easier and quicker alternative to estimate changes in canalicular volume in SCRHs.

Table 2 Effects of corrections for canalicular width and volume on changes in ITR values induced by the different treatments

	ITR (% of changes referred to control)		
	Without correction	Corrected by width	Corrected by volume
DBcAMP	+60 ± 18*	+125 ± 24*†	+153 ± 28*†
E17G	−50 ± 4*	−59 ± 4*†	−70 ± 3*†
E17G+DBcAMP	+10 ± 12#	+20 ± 13#	+3 ± 11#
TLC	−43 ± 2*	−52 ± 2*†	−60 ± 1*†
TLC+DBcAMP	−12 ± 10#	0 ± 11#	−12 ± 10#

ITR values for the different experimental groups shown in Fig. 3 were corrected by multiplying the mean of the calculated values per average canalicular width or the average canalicular volume. Both calculated and corrected ITR are presented as percentage of change, referred to their respective control

* $p < 0.05$ versus control

# $p < 0.05$ versus E17G or TLC

† $p < 0.05$ versus not corrected value

Canalicular width correctly estimates the canalicular volume and can be used to estimate biliary excretion rate in the SCRH model

Initial transport rate, calculated as described above, denotes the initial increment in canalicular concentration of the fluorescent substrate with time. Apart from depending on the rate of transport of the substrate, ITR also depends on the

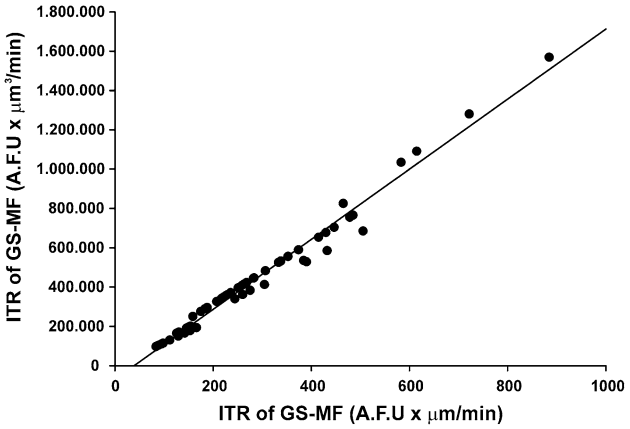

Fig. 6 Correlation between ITR values corrected by canalicular width and volume. Calculated ITR of GS-MF values (arbitrary fluorescence unit—AFU/min) were corrected by width (AFU × μm/min) and plotted against those corrected by volume (AFU × μm^3/min). Then, a regression analysis was performed. Between 20 and 30 canaliculi were measured from three independent cellular preparations. A tight correlation was recorded ($r^2 = 0.98$, $p < 0.001$)

bile volume preexisting in the lumen space; this factor is critical in our case, since the cholestatic (E17G, TLC) or choleretic (DBcAMP) agents we are dealing with have a direct influence in the canalicular volume, irrespective of the changes these compounds may have on Mrp2-mediated canalicular transport. A more appropriate measurement of canalicular transporter activity in this case is the *excretion rate* of the fluorescent substrate, which represents the *amount* (and not the *concentration*) of a substrate excreted into the biliary space per time unit. This parameter can be calculated in our system as the product of ITR by the *average canalicular volume*, or, tentatively, by its surrogate parameter, the *average canalicular width*.

Table 2 shows the percentage changes of ITR in treated SCRHs, as compared to control SCRHs. Correction of ITR by either average canalicular width or average canalicular volume significantly modified the pattern of change obtained when ITR without correction was considered in SCRHs treated with either E17G or TLC. Indeed, the percentages of decrease in ITR observed in both E17G and TLC groups were higher than those obtained without correction, reaching values that did not differ from those without correction when these groups were pre-treated with DBcAMP. The correction became critical to estimate canalicular excretion of the solute under choleretic conditions. Whereas DBcAMP alone increased ITR by 63 %, this increment was far greater when correction by width or volume were applied (+125 and +153 %, respectively).

As shown in Fig. 6, when individual ITR values belonging to all experimental groups corrected by canalicular width were plotted against those corrected by canalicular volume, a strong correlation was found ($r^2 > 0.98$; $p < 0.001$). This further confirms the feasibility of using canalicular width as a simple way to correct ITR, so as to make this parameter independent of changes in canalicular volume and to better estimate biliary excretion rate under conditions of variable bile flow.

Discussion

In this work, we provided evidence supporting the utility of SCRHs to reproduce in vitro canalicular cholestatic alterations induced by model cholestatic compounds of clinical relevance, such as E17G and TLC. Besides, choleretic and anticholestatic effects of the pro-exocytic compound DBcAMP were also readily apparent in SCRHs. This supports the use of SCRHs not only to reproduce and study cholestatic alterations, but also to investigate anticholestatic treatments or cholestatic pathomechanisms. The current evidence provided by our group and others that many forms of experimental and clinical cholestasis can be explained by the endocytic internalization of canalicular transporters relevant to bile formation, like Mrp2 used here as a model, and that this retrieval is a signaling-mediated event (Crocenzi et al. 2012), opens enormous opportunities to investigate the phenomenon at a molecular level. However, this requires stable, polarized in vitro models of bile secretion that better mimic the physiological situation. The SCRH model is ideal for this purpose, because it is the only available in vitro model employing primary cultured hepatocytes that keeps all the features of hepatocytes in situ for a period of time long enough for knockdown studies, or enough sample yield for Western blot studies (Berthiaume et al. 1996). Furthermore, human hepatocytes can be cultured in collagen-sandwich configuration and, actually, they are commercially available nowadays.

Incubation with a fluorescent substrate of a canalicular transporter such as GS-MF followed by QTLI was previously claimed to be a useful tool to detect impairment of canalicular transporter activity (Nakanishi et al. 2011). Although potentially useful for kinetic studies of function of transporters relevant to bile formation (Mrp2, in this case), the method had been only applied to an "all or nothing" condition (Mrp2-deficient Eisai hyperbilirubinemic rats), but its use in conditions of partial impairment in transport activity induced by a pathological condition, or its recovery after a proposed treatment, needed to be validated. Meticulousness of the data analysis was also limited. Transporter activity was measured as the fluorescence accumulated into the bile canaliculi until a not clearly established time point, without analyzing the influence of changes in linearity of the fluorescence signal in such an assessment. Actually, in agreement with our results (see Fig. 1), fluorescence accumulation lost linearity very shortly (4–5 min

onwards). Another critical aspect is that it relies on the measurement of the florescence intensity in the bile canaliculi, a parameter that reflects biliary concentration of the fluorescent substrate rather than its actual excretion rate. Indeed, this parameter is affected by changes in the bile flow leading to modifications of the preexisting canalicular volume; this dilutes or concentrates the solute in the canalicular lumen, thus modifying the rate of fluorescence signal increase. This is critical in cholestasis or choleresis studies. Lack of correction for an increase in canalicular volume (choleresis) would lead to underestimation of the measure of transport activity, whereas lack of correction for a decrease in canalicular volume (cholestasis) would lead to overestimation of this parameter.

To overcome these methodological drawbacks, we have proposed here a number of modifications and corrections to the approach originally reported by Nakanishi et al., so as to make it appropriated even under conditions of variable bile flow generation. First, we properly took advantage of the kinetic nature of the approach to calculate transporter activity as the initial rate of fluorescence gain (ITR) by measuring the slope of the time-course fluorescence curves during the initial linear phase, where no saturation of the transport system nor saturation of the fluorescence signal in the canalicular lumen occur. Second, we introduced a correction by the changes in the canaliculus volume by multiplying (ITR) by the *average canalicular volume*, assessed by acquiring 3D stacks of confocal SCRH images using F-actin to demark the bile canaliculus edge. Furthermore, since this is a rather time-consuming step, we successfully validated the use of the *average canalicular width* as a surrogate parameter of the canalicular volume; measurements of the canalicular width only require the acquisition of simple 2D confocal images. This assumption is based on the tight relationship obtained when both parameters were correlated (Fig. 5).

Another contribution of this work is the validation of the SCRH model for functional studies of cholestasis. For this purpose, we took advantage of two well-characterized cholestatic compounds, E17G and TLC, and we succeed in reproducing the deleterious effects that had been described in whole rats (Crocenzi et al. 2003b; Mottino et al. 2002), perfused rat livers (Beuers et al. 2001; Boaglio et al. 2010, 2012), and IRHCs (Boaglio et al. 2010, 2012; Crocenzi et al. 2003b, 2005). First, we were able to reproduce and quantify in the SCRH model the capability of both cholestatic agents to impair canalicular bile formation, as evaluated by assessing both the bile canaliculus volume and the bile canaliculus width (Table 1). Second, we were able to reproduce the capability of the cholestatic agents to inhibit Mrp2 transport function, as assessed by ITR of GS-MF; interestingly, the decrease in ITR of GS-MF in SCRHs treated with 200 μM E17G and 2.5 μM TLC (50 and 43 %, respectively) were of similar magnitude to that reported for canalicular vacuolar accumulation of GS-MF in IRHCs (Boaglio et al. 2010; Crocenzi et al. 2005). Third, we were able to visualize the endocytic internalization of Mrp2 induced by both cholestatic agents, a main pathomechanism involved in their cholestatic effects (Crocenzi et al. 2012). Finally, we reproduced in the SCRH model the capability of the anticholestatic compound DBcAMP to revert all these cholestatic manifestations. Furthermore, the well-known choleretic effects of DBcAMP when administered alone were readily apparent from the increase in the canalicular volume/width values (see Table 1); this choleretic effect is associated in part with the capability of cAMP to increase Mrp2 activity, a property that could be reproduced here as well by measuring ITR of GS-MF (see Table 2). These latter results demonstrate that the SCRH model can be also used for studies on the mechanisms of choleresis.

In conclusion, our results clearly support the utility of SCRHs as an in vitro model for the study of changes in canalicular bile formation induced by either choleretic or cholestatic compounds. We have also provided here a way to quantify changes in canalicular bile flow generation and activity of canalicular transporters involved in this phenomenon. Finally, we have reproduced and visualized in the SCRH model a main mechanism by which cholestatic compounds induce biliary secretory failure, i.e., the endocytic internalization of canalicular transporters. There is an increasing demand for well-characterized and efficient in vitro models for studies of polarized hepatocellular transport at a molecular level under both physiological and physiopathological conditions. With the methodological approach provided here, the SCRH model may become the method of choice for this purpose.

Acknowledgments This work was supported by Grants from the Agencia Nacional de Promoción Científica y Tecnológica (ANPCyT, PICT 2010 No. 0995) and Consejo Nacional de Investigaciones Científicas y Técnicas (CONICET, PIP No. 00691). The authors wish to thank J. Elena Ochoa, M. D., and Mr. Diego Taborda for technical assistance in isolation of hepatocytes, and Dr. María Cecilia Larocca for expert advice in confocal image analysis.

References

Ansede JH, Smith WR, Perry CH, St Claire RL, Brouwer KR (2010) An in vitro assay to assess transporter-based cholestatic hepatotoxicity using sandwich-cultured rat hepatocytes. Drug Metab Dispos 38(2):276–280. doi:10.1124/dmd.109.028407

Barosso IR, Zucchetti AE, Boaglio AC et al (2012) Sequential activation of classic PKC and estrogen receptor alpha is involved in estradiol 17ß-D-glucuronide-induced cholestasis. PLoS One 7(11):e50711. doi:10.1371/journal.pone.0050711

Berthiaume F, Moghe PV, Toner M, Yarmush ML (1996) Effect of extracellular matrix topology on cell structure, function, and

physiological responsiveness: hepatocytes cultured in a sandwich configuration. FASEB J 10(13):1471–1484

Beuers U, Probst I, Soroka C, Boyer JL, Kullak-Ublick GA, Paumgartner G (1999) Modulation of protein kinase C by taurolithocholic acid in isolated rat hepatocytes. Hepatology 29(2):477–482. doi:10.1002/hep.510290227

Beuers U, Bilzer M, Chittattu A et al (2001) Tauroursodeoxycholic acid inserts the apical conjugate export pump, Mrp2, into canalicular membranes and stimulates organic anion secretion by protein kinase C-dependent mechanisms in cholestatic rat liver. Hepatology 33(5):1206–1216. doi:10.1053/jhep.2001.24034

Beuers U, Denk GU, Soroka CJ et al (2003) Taurolithocholic acid exerts cholestatic effects via phosphatidylinositol 3-kinase-dependent mechanisms in perfused rat livers and rat hepatocyte couplets. J Biol Chem 278(20):17810–17818. doi:10.1074/jbc.M209898200

Boaglio AC, Zucchetti AE, Sanchez Pozzi EJ et al (2010) Phosphoinositide 3-kinase/protein kinase B signaling pathway is involved in estradiol 17ß-D-glucuronide-induced cholestasis: complementarity with classical protein kinase C. Hepatology 52(4):1465–1476. doi:10.1002/hep.23846

Boaglio AC, Zucchetti AE, Toledo FD et al (2012) ERK1/2 and p38 MAPKs are complementarily involved in estradiol 17ß-D-glucuronide-induced cholestasis: crosstalk with cPKC and PI3K. PLoS One 7(11):e49255. doi:10.1371/journal.pone.0049255

Boyer JL, Soroka CJ (1995) Vesicle targeting to the apical domain regulates bile excretory function in isolated rat hepatocyte couplets. Gastroenterology 109(5):1600–1611. doi:10.1016/0016-5085(95)90649-5

Coleman R, Roma MG (2000) Hepatocyte couplets. Biochem Soc Trans 28(2):136–140

Crocenzi FA, Mottino AD, Cao J et al (2003a) Estradiol-17ß-D-glucuronide induces endocytic internalization of Bsep in rats. Am J Physiol Gastrointest Liver Physiol 285(2):G449–G459. doi:10.1152/ajpgi.00508.2002

Crocenzi FA, Mottino AD, Sanchez Pozzi EJ et al (2003b) Impaired localisation and transport function of canalicular Bsep in taurolithocholate-induced cholestasis in the rat. Gut 52(8):1170–1177. doi:10.1136/gut.52.8.1170

Crocenzi FA, Basiglio CL, Perez LM, Portesio MS, Sanchez Pozzi EJ, Roma MG (2005) Silibinin prevents cholestasis-associated retrieval of the bile salt export pump, Bsep, in isolated rat hepatocyte couplets: possible involvement of cAMP. Biochem Pharmacol 69:1113–1120. doi:10.1016/j.bcp.2005.01.009

Crocenzi FA, Sanchez Pozzi EJ, Ruiz ML et al (2008) Ca(2+)-dependent protein kinase C isoforms are critical to estradiol 17beta-D-glucuronide-induced cholestasis in the rat. Hepatology 48(6):1885–1895. doi:10.1002/hep.22532

Crocenzi FA, Zucchetti AE, Boaglio AC et al (2012) Localization status of hepatocellular transporters in cholestasis. Front Biosci 17:1201–1218. doi:10.2741/3981

Cruz LN, Guerra MT, Kruglov E et al (2010) Regulation of multidrug resistance-associated protein 2 by calcium signaling in mouse liver. Hepatology 52(1):327–337. doi:10.1002/hep.23625

De Bruyn T, Chatterjee S, Fattah S et al (2013) Sandwich-cultured hepatocytes: utility for in vitro exploration of hepatobiliary drug disposition and drug-induced hepatotoxicity. Expert Opin Drug Metab Toxicol 9(5):589–616. doi:10.1517/17425255.2013.773973

Dunn JC, Yarmush ML, Koebe HG, Tompkins RG (1989) Hepatocyte function and extracellular matrix geometry: long-term culture in a sandwich configuration. FASEB J 3(2):174–177

Dunn JC, Tompkins RG, Yarmush ML (1991) Long-term in vitro function of adult hepatocytes in a collagen sandwich configuration. Biotechnol Prog 7(3):237–245. doi:10.1021/bp00009a007

Dunn JC, Tompkins RG, Yarmush ML (1992) Hepatocytes in collagen sandwich: evidence for transcriptional and translational regulation. J Cell Biol 116(4):1043–1053. doi:10.1083/jcb.116.4.1043

Fouin-Fortunet H, Le Quernec L, Erlinger S, Lerebours E, Colin R (1982) Hepatic alterations during total parenteral nutrition in patients with inflammatory bowel disease: a possible consequence of lithocholate toxicity. Gastroenterology 82(5 Pt 1):932–937

Garcia F, Kierbel A, Larocca MC et al (2001) The water channel aquaporin-8 is mainly intracellular in rat hepatocytes, and its plasma membrane insertion is stimulated by cyclic AMP. J Biol Chem 276(15):12147–12152. doi:10.1074/jbc.M009403200

Gautam A, Ng OC, Strazzabosco M, Boyer JL (1989) Quantitative assessment of canalicular bile formation in isolated hepatocyte couplets using microscopic optical planimetry. J Clin Invest 83(2):565–573. doi:10.1172/JCI113919

Kipp H, Pichetshote N, Arias IM (2001) Transporters on demand: intrahepatic pools of canalicular ATP binding cassette transporters in rat liver. J Biol Chem 276(10):7218–7224. doi:10.1074/jbc.M007794200

Kruglov EA, Gautam S, Guerra MT, Nathanson MH (2011) Type 2 inositol 1,4,5-trisphosphate receptor modulates bile salt export pump activity in rat hepatocytes. Hepatology 54(5):1790–1799. doi:10.1002/hep.24548

Larocca MC, Soria LR, Espelt MV, Lehmann GL, Marinelli RA (2009) Knockdown of hepatocyte aquaporin-8 by RNA interference induces defective bile canalicular water transport. Am J Physiol Gastrointest Liver Physiol 296(1):G93–G100. doi:10.1152/ajpgi.90410.2008

Linarelli LG, Williams CN, Phillips MJ (1972) Byler's disease: fatal intrahepatic cholestasis. J Pediatr 81(3):484–492. doi:10.1016/S0022-3476(72)80174-4

Liu X, LeCluyse EL, Brouwer KR et al (1999) Biliary excretion in primary rat hepatocytes cultured in a collagen-sandwich configuration. Am J Physiol Gastrointest Liver Physiol 277(1 Pt 1):G12–G21

Milkiewicz P, Roma MG, Mills CO, Coleman R, Elias E (1999) Tauroursodeoxycholate (TUDCA) protects against redistribution of multidrug resistant protein 2 (Mrp2) and disruption of F-actin caused by taurolithocholate (TLC); a study in isolated rat hepatocyte couplets. Hepatology 30(4 Pt 2):462A

Milkiewicz P, Roma MG, Elias E, Coleman R (2002a) Hepatoprotection with tauroursodeoxycholate and β-muricholate against taurolithocholate induced cholestasis: involvement of signal transduction pathways. Gut 51(1):113–119. doi:10.1136/gut.51.1.113

Milkiewicz P, Roma MG, Elias E, Coleman R (2002b) Pathobiology and experimental therapeutics in hepatocellular cholestasis: lessons from the hepatocyte couplet model. Clin Sci (Lond) 102(6):603–614. doi:10.1042/CS20010353

Mottino AD, Cao J, Veggi LM, Crocenzi FA, Roma MG, Vore M (2002) Altered localization and activity of canalicular Mrp2 in estradiol-17ß-D-glucuronide-induced cholestasis. Hepatology 35(6):1409–1419. doi:10.1053/jhep.2002.33327

Murphy GM, Jansen FH, Billing BH (1972) Unsaturated monohydroxy bile acids in cholestatic liver disease. Biochem J 129(2):491–494

Nakanishi T, Shibue Y, Fukuyama Y et al (2011) Quantitative time-lapse imaging-based analysis of drug–drug interaction mediated by hepatobiliary transporter, multidrug resistance-associated protein 2, in sandwich-cultured rat hepatocytes. Drug Metab Dispos 39(6):984–991. doi:10.1124/dmd.111.038059

Roelofsen H, Soroka CJ, Keppler D, Boyer JL (1998) Cyclic AMP stimulates sorting of the canalicular organic anion transporter (Mrp2/cMoat) to the apical domain in hepatocyte couplets. J Cell Sci 111(Pt 8):1137–1145

Roma MG, Penalva GL, Aguero RM, Rodriguez Garay EA (1994) Hepatic transport of organic anions in taurolithocholate-induced cholestasis in rats. J Hepatol 20(5):603–610. doi:10.1016/S0168-8278(05)80347-2

Roma MG, Milkiewicz P, Elias E, Coleman R (2000) Control by signaling modulators of the sorting of canalicular transporters in rat hepatocyte couplets: role of the cytoskeleton. Hepatology 32(6):1342–1356. doi:10.1053/jhep.2000.20519

Roma MG, Crocenzi FA, Sanchez Pozzi EA (2008) Hepatocellular transport in acquired cholestasis: new insights into functional, regulatory and therapeutic aspects. Clin Sci (Lond) 114(9):567–588. doi:10.1042/CS20070227

Schonhoff CM, Webster CR, Anwer MS (2013) Taurolithocholate-induced MRP2 retrieval involves MARCKS phosphorylation by protein kinase C in HUH-NTCP Cells. Hepatology 58(1):284–292. doi:10.1002/hep.26333

Setchell KD, Schwarz M, O'Connell NC et al (1998) Identification of a new inborn error in bile acid synthesis: mutation of the oxysterol 7alpha-hydroxylase gene causes severe neonatal liver disease. J Clin Invest 102(9):1690–1703. doi:10.1172/JCI2962

Swift B, Pfeifer ND, Brouwer KL (2010) Sandwich-cultured hepatocytes: an in vitro model to evaluate hepatobiliary transporter-based drug interactions and hepatotoxicity. Drug Metab Rev 42(3):446–471. doi:10.3109/03602530903491881

Tsukada N, Ackerley CA, Phillips MJ (1995) The structure and organization of the bile canalicular cytoskeleton with special reference to actin and actin-binding proteins. Hepatology 21(4):1106–1113. doi:10.1002/hep.1840210433

Vore M, Liu Y, Huang L (1997) Cholestatic properties and hepatic transport of steroid glucuronides. Drug Metab Rev 29(1–2):183–203. doi:10.3109/03602539709037580

Wilton JC, Coleman R, Lankester DJ, Chipman JK (1993) Stability and optimization of canalicular function in hepatocyte couplets. Cell Biochem Funct 11:179–185. doi:10.1002/cbf.290110305

Zucchetti AE, Barosso IR, Boaglio AC et al (2013) G protein-coupled receptor 30-adenylyl cyclase-protein kinase A pathway is involved in estradiol 17β-D-glucuronide-induced cholestasis. Hepatology. doi:10.1002/hep.26752